



Clinical characteristics and associated factors of pediatric acute necrotizing encephalopathy: a retrospective study

Huiling Zhang, MA¹, Yilong Wang, PhD¹, Qianyun Ding, MA¹, Xuekun Li, PhD^{1,2}, Sheng Ye, PhD¹

¹Children's Hospital, Zhejiang University School of Medicine, National Clinical Research Center for Child Health, Hangzhou, Zhejiang, China; ²The Institute of Translational Medicine, School of Medicine, Zhejiang University, Hangzhou, China

Background: In the clinic, pediatric acute necrotizing encephalopathy (ANE) primarily affects children under 5 years of age and is characterized by severe brain damage and high mortality. However, some challenges remain regarding the diagnosis and treatment of ANE. In the present study, we analyzed the clinical characteristics and related factors of ANE with the aim of providing improved diagnostic and treatment strategies.

Purpose: The main purpose of this study is to gain a deeper understanding of the clinical characteristics and pathophysiology of ANE through a retrospective study, and to provide clinical practitioners with more effective diagnostic and treatment strategies to improve patient survival rates and quality of life.

Methods: Thirty-four pediatric ANE patients admitted to Zhejiang University School of Medicine Hospital between February 2019 and December 2023 were included in this study. To identify the factors associated with mortality, clinical, laboratory and imaging data were analyzed with independent-sample *t* tests, Mann-Whitney *U* tests, Fisher exact probability tests and receiver operating characteristic curve analyses.

Results: In this cohort of 34 patients, the most common symptoms were fever, seizures, altered consciousness, vomiting, diarrhea and shock. The mortality rate was 55.9%. Laboratory tests revealed that patients who died had higher creatinine, lactate, activated partial thromboplastin time, thrombin time, interleukin (IL)-6, IL-10, creatine kinase, and D-dimer than survivors. Imaging examinations predominantly revealed symmetrical lesions in the thalamus. The fatal group displayed lower Glasgow Coma Scale (GCS) scores and severe complications. Other factors related to mortality included the arterial pH, GCS score and hospitalization duration.

Conclusion: The most common symptoms of ANE are fever, seizures, altered consciousness, vomiting, diarrhea and shock, and ANE has a high mortality rate. The GCS score and arterial pH are critical biomarkers for assessing the severity of ANE.

Key words: Acute necrotizing encephalopathy, Mortality, Clinical characteristics

Key message

- The mortality rate of acute necrotizing encephalopathy was high.
- Laboratory tests revealed that the fatal group had higher creatinine, lactate, activated partial thromboplastin time, thrombin time, interleukin (IL)-6, IL-10, creatine kinase, and D-dimer than survivors.
- The fatal group displayed lower Glasgow Coma Scale scores and arterial pH.

Introduction

Pediatric acute necrotizing encephalopathy (ANE) is a rare and fatal disease that typically affects children under 5 years of age. ANE is frequently induced by viral infections and manifests as fever, seizures, altered consciousness, and bilateral thalamic damage.^{1,2)} ANE progresses rapidly and has a high occurrence in the winter.³⁾ Various pathogens, such as influenza A, severe acute respiratory syndrome coronavirus 2 (SARS-CoV-2), human herpes virus 6/7, parainfluenza, rotavirus, herpes simplex virus, Avarice-Zoster virus, Epstein-Barr virus, Zika virus and rotavirus, are implicated in the onset of ANE.⁴⁻¹¹⁾

Corresponding author: Sheng Ye. Children's Hospital, Zhejiang University School of Medicine, National Clinical Research Center for Child Health, Hangzhou, Zhejiang, China

✉ Email: yeshengchina@zju.edu.cn, <https://orcid.org/0000-0003-2201-0261>

Co-corresponding author: Xuekun Li. Children's Hospital, Zhejiang University School of Medicine, National Clinical Research Center for Child Health, Hangzhou, Zhejiang, China

✉ Email: xuekun_li@zju.edu.cn, <https://orcid.org/0000-0002-6985-6363>

Received: 9 May 2024, Revised: 26 July 2024, Accepted: 27 July 2024

This is an open-access article distributed under the terms of the Creative Commons Attribution Non-Commercial License (<http://creativecommons.org/licenses/by-nc/4.0/>) which permits unrestricted non-commercial use, distribution, and reproduction in any medium, provided the original work is properly cited.

Copyright © 2025 by The Korean Pediatric Society

The pathogenesis of ANE remains unclear, with hypotheses focused on immune responses, genetic factors, and metabolic pathways. Immune responses, characterized by the release of proinflammatory mediators such as interleukin-6 (IL-6), tumor necrosis factor-alpha (TNF- α), and interferon-gamma (IFN- γ),¹²⁻¹⁴ along with the activation of CD⁴⁺ T cells, CD⁸⁺ T cells, and B cells,^{15,16} contribute to excessive inflammatory reactions and neuronal damage. This phenomenon, often referred to as the "cytokine storm," leads to cerebral edema, petechial hemorrhage, and necrosis by disrupting the blood-brain barrier (BBB).¹⁷

Routine laboratory examination often reveals elevated serum transaminase, creatine kinase (CK), and lactate dehydrogenase (LDH) levels, and hypoglycemia and nitrogenous metabolic acidosis may also occur. Disseminated intravascular coagulation (DIC), which is characterized by changes in fibrinolytic products, platelet count, prothrombin time, and fibrinogen levels, may result from severe instances. Cerebrospinal fluid (CSF) analysis typically reveals increased protein levels with normal cell counts.¹⁸ Standardized criteria for ANE diagnosis are lacking, but radiological findings often reveal multifocal and symmetric lesions extending to various brain regions, including the brainstem, white matter, basal ganglia, cerebellum, corpus callosum, and hippocampus.

Currently, the diagnosis of ANE lacks of standardized criteria and is mainly based on information in case reports, and its pathogenesis remains unclear. With no specific treatment available, early identification, immunotherapy, and symptomatic support remain fundamental in clinical management. In our retrospective study, conducted at Zhejiang University School of Medicine Hospital, we analyzed data from 34 pediatric ANE patients, aiming to refine diagnostic and treatment strategies by elucidating clinical characteristics and associated factors.

Methods

1. Study design

In this retrospective study, we analyzed the clinical presentations, laboratory parameters, treatment protocols, and prognostic follow-ups of 34 pediatric ANE patients admitted to Zhejiang University School of Medicine Hospital between February 2019 and December 2023. Individual informed consent was deemed unnecessary given that we collected data from published sources rather than conducting direct biomedical research on individuals. The Glasgow Coma Scale (GCS) was used to assess consciousness levels on admission, with scores

ranging from 15 points (normal) to <8 points (coma) divided into gradations of mild and moderate consciousness impairment.

The studies involving humans were approved by the Medical Ethics Committee of the Children's Hospital, Zhejiang University School of Medicine (2024-IRB-0151-P-01). The studies were conducted in accordance with local legislation and institutional requirements. Written informed consent from the patients/participants or patients'/participants' legal guardian/next of kin was not required for this study in accordance with the national legislation and the institutional requirements.

2. Patients

Thirty-four patients were diagnosed with ANE at the Children's Hospital, Zhejiang University School of Medicine, between February 2019 and December 2023. The diagnostic criteria for ANE, adapted from Neilson et al., included the following: (1) acute encephalopathy, appearing 1-3 days after the onset of febrile illness and characterized by consciousness deterioration (coma) and seizures; (2) brain imaging revealing symmetric, multifocal lesions in specific regions, including bilaterally in the thalamus and periventricular white matter; (3) absence of CSF pleocytosis, with an increase in CSF protein; (4) variable presence of elevated serum transaminase; and (5) normal ammonia levels.^{1,19} Other diseases were excluded, including infectious diseases, autoimmune, metabolic, and toxic diseases, such as acute disseminated encephalomyelitis, toxic shock syndrome, Reyes syndrome, Leigh syndrome, acute hemorrhagic leukoencephalopathy, and various causes of symmetrical bilateral basal ganglia necrotic diseases (such as carbon monoxide, methanol, cyanide, carbamazepine poisoning, etc.).

3. Data collection

Nasopharyngeal swabs from patients were tested for various viruses, including influenza A and B, parainfluenza, adenovirus, chlamydia, rhinovirus, metapneumovirus, coronavirus, respiratory syncytial virus, *Mycoplasma pneumoniae*, bocavirus and SARS-CoV-2, with real-time polymerase chain reaction. Blood cultures were performed to exclude septicemia. Clinical data, including demographic information, symptoms, treatment details, and length of hospital stay, were meticulously collected. Blood and CSF parameters, which included routine parameters, alanine aminotransferase (ALT), aspartate aminotransferase (AST), albumin, bilirubin, LDH, CK, serum creatinine, urea nitrogen, pH, lactate, blood sodium, blood calcium, blood glucose, procalcitonin (PCT), activated partial thromboplastin time (APTT), proth-

rombin time, fibrinogen, D-dimer, erythrocyte sedimentation rate, ferritin, blood ammonia, cytokines (IL-6, IL-10, TNF- α , IFN- γ), and indicators of cell-mediated immunity (CD3, CD4, CD8, CD19, CD4/CD8), were collected retrospectively from patients who underwent laboratory examinations upon hospitalization. Head magnetic resonance imaging (3.0T MRI, including T1-weighted imaging, T2-weighted imaging, and fluid-attenuated inversion recovery [FLAIR]) or computed tomography

(CT) were performed, and the images were analyzed by experienced pediatric radiologists.

4. Statistical analysis

Data processing was conducted with Python software, and the data are presented as the means \pm standard deviations. For normally distributed quantitative data, independent-sample *t* tests were used for intergroup comparisons, while the independent-sample Mann-Whitney

Table 1. Demographic and clinical features of acute necrotizing encephalopathy patients (n=34)

Variable	All (n=34)	Survival group (n=15)	Fatal group (n=19)	P value
Male sex	22 (64.7)	11 (73.3)	11 (57.9)	0.476
Age (mo)	46.47 \pm 5.77	40.67 \pm 33.38	51.05 \pm 33.99	0.379
Symptoms and signs				
Fever	34 (100)	15 (100)	19 (100)	>0.999
Body temperature peak (°C)	40.51 \pm 0.19	40.41 \pm 0.99	40.58 \pm 1.19	0.646
Diarrhea	8 (23.5)	4 (26.7)	4 (21.1)	>0.999
Vomiting	11 (32.3)	5 (33.3)	6 (31.6)	>0.999
Convulsions	31 (91.2)	13 (86.7)	18 (94.7)	>0.999
Onset time of consciousness disorder (day)	1.52 \pm 1.61	1.77 \pm 2.15	1.33 \pm 1.03	0.437
Status epilepticus	16 (51.6)	9 (60.0)	7 (36.8)	0.190
GCS score	6.0 \pm 0.63	7.60 \pm 3.58	4.74 \pm 3.33	0.024
Shock	13 (38.2)	3 (20.0)	10 (52.6)	0.079
Vasoactive drugs	14 (41.2)	2 (13.3)	12 (63.1)	0.005
Decerebrate or decorticate posture	13 (38.2)	0 (0)	13 (68.4)	<0.05
Positive Babinski sign	12 (35.3)	7 (46.7)	5 (26.3)	0.288
Underlying disease	1 (2.9)	0 (0)	1 (5.3)	-
History of previous convulsion	5 (14.7)	1 (6.7)	4 (21.1)	-
Complication				
Gastrointestinal hemorrhage	6 (17.6)	0 (0)	6 (31.6)	0.024
Pneumorrhagia	6 (17.6)	1 (6.7)	5 (26.3)	0.196
Liver damage	33 (97.1)	15 (100)	18 (94.7)	>0.999
AKI	12 (35.3)	1 (6.7)	11 (57.9)	0.003
Albuminuria	14 (41.2)	3 (20.0)	11 (57.9)	0.038
Genetic metabolic profile	18 (52.9)	10 (80.0)	8 (42.1)	0.728
Heart failure	8 (23.5)	0 (0)	8 (42.1)	0.005
DIC	13 (38.2)	1 (6.7)	12 (63.2)	<0.05
Hospitalization duration	6.74 \pm 5.65	10.93 \pm 3.31	3.42 \pm 4.87	<0.05
Etiological detection				
FA	23 (67.6)	9 (60.0)	14 (73.7)	0.692
FB	2 (5.9)	0 (0)	2 (10.5)	0.492
SARS-CoV-2	3 (8.8)	3 (20.0)	0 (0)	0.187
Adenovirus	1 (2.9)	0 (0)	1 (5.3)	>0.999
Rhinovirus	1 (2.9)	0 (0)	1 (5.3)	>0.999
Unclear	4 (11.9)	2 (13.3)	2 (10.5)	0.187
Symptomatic support therapy				
Hormones (10–30 mg/kg/day)	32 (94.1)	15 (100)	17 (89.5)	0.492
Gamma globulin	34 (100)	15 (100)	19 (100)	>0.999
Advanced life support				
Mechanical ventilation	26 (76.5)	7 (46.7)	19 (100)	<0.05
Plasma exchange	2 (5.9)	1 (6.7)	1 (5.3)	>0.999
Decompressive craniectomy	2 (5.9)	1 (6.7)	1 (5.3)	>0.999

Values are presented as number (%) or mean \pm standard deviation.

GCS, Glasgow Coma Scale; AKI, acute kidney injury; DIC, disseminated intravascular coagulation; FA, influenza A; FB, influenza B; SARS-CoV-2, severe acute respiratory syndrome coronavirus 2.

Boldface indicates a statistically significant difference with *P*<0.05.

U test was used for nonnormally distributed data. The data are expressed as percentages, and intergroup comparisons were performed using the chi-square test or Fisher exact test. Receiver operating characteristic (ROC) curve analysis was used to identify statistically significant indicators to determine the optimal threshold for group comparison. Single-factor logistic regression analysis was used to compute odds ratios to assess relative risk, with a 2-sided *P* value <0.05 indicating statistical significance.

Results

1. Patient characteristics

A total of 34 ANE patients, 22 males and 12 females, were included in the present study. The majority (70.6%) were under 5 years old, with an average age of 46 months. Among the 34 patients, 25 patients (73.5%) were positive for seasonal influenza A or B. There were 18 cases (52.9%) occurring in winter and 10 cases (29.4%) occurring in spring. Patients were divided into survival (*n*=15) and death (*n*=19) groups based on their outcomes. The mortality rate was 55.9%. Notably, 5 patients had a history of febrile seizure. One patient had a diagnosis of nephrotic syndrome and allergic asthma, and 1 patient was a premature infant. All patients had achieved normal developmental milestones, and their parents were reported to be in good health.

2. Clinical presentation

All patients with ANE had fever, seizures and altered consciousness upon admission. Detailed information can be found in Table 1. All admitted children exhibited persistent fever prior to admission, with a mean peak temperature of 40.5°C. Within 1.5 days of fever onset, 76.5% of patients displayed consciousness impairment. Among seizure patients, 51.6% progressed to status epilepticus. GCS scores indicated varying degrees of impairment, from mild (1 of 34) to moderate (9 of 34) and coma (24 of 34). Multiple organ failure (MOF) primarily manifested as liver dysfunction (33 of 34). A total of 76.5% of patients underwent ventilation, 2 patients required tracheotomy, 2 patients underwent plasma exchange, and 2 patients underwent comprehensive tonsillectomy. Compared with the survival group, the fatal group showed more frequent decorticate or decerebrate postures and had longer hospital stays and greater use of vasoactive medications (*P*<0.05).

3. Laboratory findings

Elevated serum enzyme levels, including AST and ALT, were observed in 82.4% of patients, along with increased PCT levels in 94.1% of patients and metabolic acidosis in 67.6% of patients. Elevated blood lactate concentrations were noted in 79.4% of the patients, as depicted in Table 2. In the analysis of cell-mediated immunity in only 24 patients, the activation of CD19+ T cells (B lymphocytes) was observed in 23 patients, while decreased levels of CD3, CD4, and CD8 (T lymphocytes) were noted in 20 patients, suggesting immune dysfunction and a potential decline in T-cell activation. However, these markers exhibited no statistically significant differences in be-

Table 2. Laboratory examination parameters of acute necrotizing encephalopathy patients (n=34)

Parameter	Survival group (n=15)	Fatal group (n=19)	<i>P</i> value
Serum creatinine (μmol/L) (ref: 13–33)	49.27±27.13	85.22±57.84	0.024
Lactic acid (mmol/L) (ref: 0.5–1.6)	2.2±1.12	5.99±4.54	0.003
pH (ref: 7.35–7.45)	7.35±0.05	7.22±0.18	0.006
APTT (sec) (ref: 23–38)	33.42±11.43	56.82±27.66	0.003
Cytokine (n=29)			
IL-6 (pg/mL) (ref: 1.7–16.6)	316.23±581.25	6,619.42±9,268.70	0.01
IL-10 (pg/mL) (ref: 2.6–4.9)	129.03±141.31	693.24±762.49	0.007
TNF-α (pg/mL) (ref: 0.1–5.2)	1.99±0.83	3.02±2.27	0.094
IFN-γ (pg/mL) (ref: 1.1–17.3)	5.24±4.59	6.95±8.73	0.495
Other biochemical detection (n=31)			
CK (U/L) (ref: 39–308)	169.93±152.95	374.94±283.54	0.021
Other items of coagulation function (n=30)			
TT (sec) (ref: 15.0–22.0)	23.75±7.09	39.65±26.07	0.037
D-dimer (mg/L) (ref: <0.55)	11.73±9.49	78.02±101.06	0.024

Values are presented as mean±standard deviation.

APTT, activated partial thrombin time; IL-6, interleukin-6; IL-10, interleukin-10; TNF-α, tumor necrosis factor-alpha; IFN-gamma, interferon-gamma; CK, creatine kinase; TT, thrombin time.

Boldface indicates a statistically significant difference with *P*<0.05.

Table 3. Cerebrospinal fluid (CSF) examination parameters (n=13)

Parameter	Mean±SD	P value
CSF white blood cell counts (*10 ⁶ /L)	1.93±0.33	0.85
CSF lactate dehydrogenase (U/L)	125.60±39.65	0.56
CSF glucose (mmol/L)	5.16±0.59	0.47
CSF micro total protein (mg/L)	2,860.0±967.7	0.55
Creatine kinase (U/L)	27.25±21.33	0.41
Chloride ion (mmol/L)	26.58±6.32	0.68
Adenosine deaminase (U/L)	0.88±0.77	0.79

SD, standard deviation.

Table 4. Imaging examinations findings

Findings	Number
Preadmission 24-hour cranial CT examination: edema	12
Preadmission 24-hour cranial CT examination: no abnormalities	9
Distribution of lesions of MRI within 1 week (n=19)	
Thalamus and internal capsule and Basal ganglia region	19
Cerebral white matter	12
Involvement of the cerebellar hemispheres, hippocampus, and other regions	10
Brainstem and/or midbrain	12
Residual lesions after 1 week (n=11)	
Thalamic hemorrhage	4

CT, computed tomography; MRI, head magnetic resonance imaging.

tween-group comparisons.

Primary complications in the fatal group included gastrointestinal hemorrhage, acute kidney injury, heart failure, DIC, and albuminuria ($P<0.05$). Compared with the survival group, the fatal group also exhibited increased IL-6 (6,619.0 pg/mL vs. 316.2 pg/mL, $P=0.01$), IL-10 (693.3 pg/mL vs. 129.0 pg/mL, $P=0.007$), serum creatinine (85.2 μ mol/L vs. 49.3 μ mol/L, $P=0.024$), CK (374.9 U/L vs. 173.5 U/L, $P=0.021$), lactate (6.0 mmol/L vs. 2.2 mmol/L, $P=0.003$), APTT (56.8 seconds vs. 33.4 seconds, $P=0.003$), TT (39.7 seconds vs. 23.8 seconds, $P=0.037$), and D-dimer (78.0 mg/L vs. 11.7 mg/L, $P=0.024$). In addition, the fatal group had lower pH values (7.2 vs. 7.4, $P=0.006$) and GCS scores (4.7 vs. 7.6, $P=0.024$) than did the survival group.

CSF analysis was performed for 15 patients (44.1%) (Table 3) and revealed increased protein levels in 13 patients and elevated LDH levels in 8 patients, while white cell counts did not change among the patients. The results of CSF pathogen detection were negative, suggesting no direct evidence of pathogen invasion.

4. Imaging and electroencephalography

Among the 34 patients, 33 patients underwent cranial CT scans, and 1 patient was unable to complete this pro-

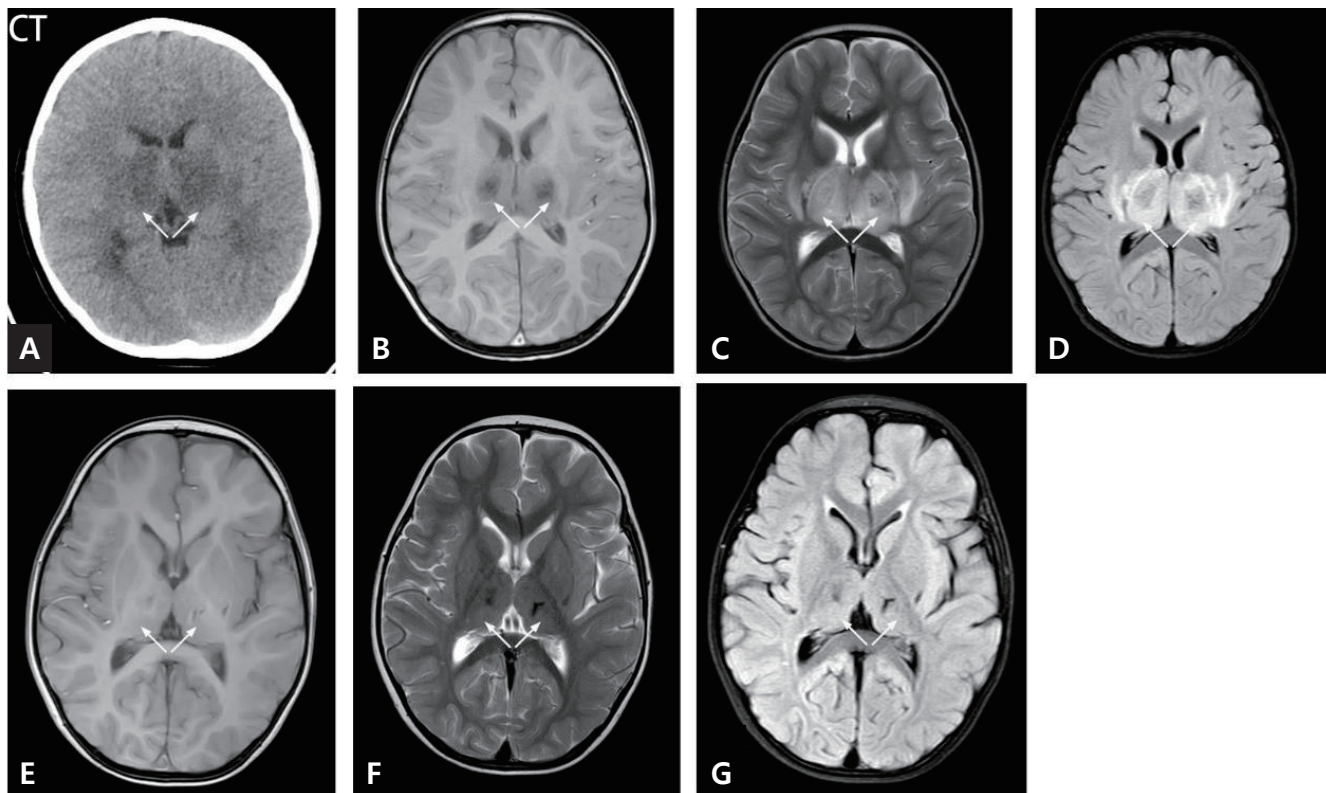


Fig. 1. A 2-year-old boy presented with acute necrotizing encephalitis. (A) The thalamus exhibited swelling, as observed in the computed tomography (CT) scan. Bilaterally, the thalamus showed high T2WI signal intensity, central low signal areas, and slightly increased signal intensity on T2WI/FLAIR images (white arrow) (B, T1WI; C, T2WI; D, T2WI/FLAIR). Three months later, a follow-up brain MRI revealed bilateral slightly increased T2WI/FLAIR signals in the thalamus, with central low signal areas. Residual softening lesions and deposition of hemosiderin in the thalami were observed (white arrow) (E, T1WI; F, T2WI; G, T2WI/FLAIR). T2WI, T2-weighted image; T1WI, T1-weighted image; FLAIR, fluid-attenuated inversion recovery.

cedure due to unstable clinical conditions. Imaging analysis revealed signs of cerebral edema (Table 4). Of the 33 patients who underwent cranial CT within 24 hours before admission, 21 displayed cerebral edema. Upon admission, 9 patients showed no apparent lesions, but symmetrical lesions were later identified bilaterally in the thalamus and other regions during reexamination (1-2 days after the initial scan). Cranial CT results typically revealed bilateral thalamus hypodensity and signs of cerebral edema (Fig. 1A).

Cranial MRIs revealed typical thalamic symmetric involvement (Figs. 1B-D and 2B-D) in various regions, such as the basal ganglia (17 of 33), brainstem and midbrain (23 of 33), bilaterally in the cerebral hemisphere (frontal, parietal, temporal, occipital lobes) gray and white mat-

ter (24 of 33), cerebellar hemisphere gray and white matter, and hippocampus (20 of 33). In total, 19 patients underwent cranial MRI, which revealed abnormally high signals on T1-weighted images (T1WIs) with a concentric ring shape in the central thalamus and low signals around it, while T2-weighted images (T2WIs) showed high signals. White matter damage exhibited low signals on T1WI and high signals on T2WI, with lesions involving the basal ganglia, brainstem, cortex, and white matter. Hemorrhage appeared in 4 patients (21.1%) at different stages of cranial CT/MRI (Fig. 2E-G). Only 2 patients had follow-up MRI data 3 months after disease onset. One child had white matter demyelination with signs of cerebral atrophy (Fig. 1E-G), while the other had bilateral residual softening lesions in the thalamus and

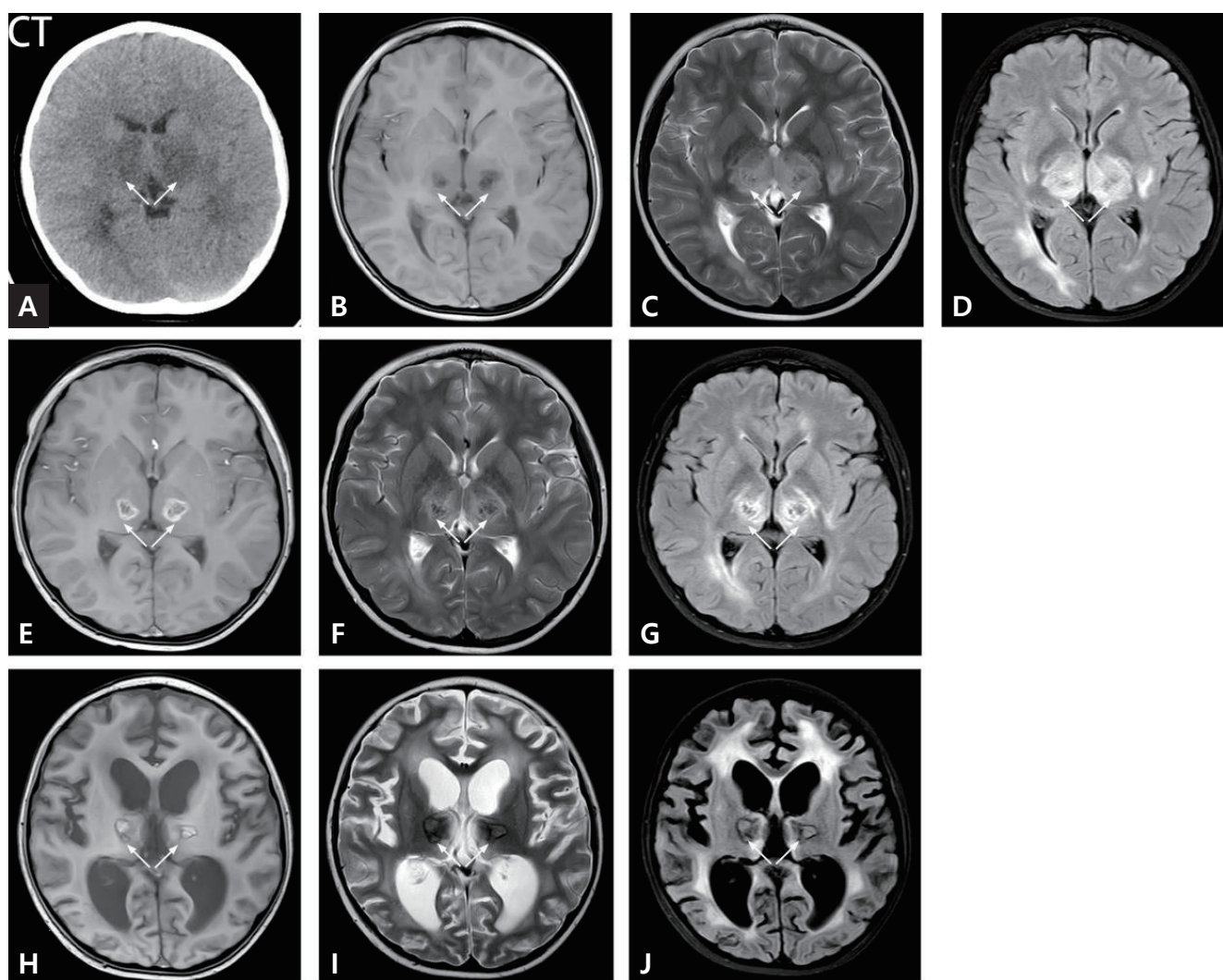


Fig. 2. An 8-year-old boy presented with acute necrotizing encephalitis. (A) The thalamus exhibited significant swelling, as evidenced by a sheet-like area of low density on computed tomography (CT) scan. Both thalami displayed symmetrical enlargement, with T2WIs indicating high signal intensity and slightly increased density on T2WI/FLAIR sequences (white arrow) (B, T1WI; C, T2WI; D, T2WI/FLAIR). In a subsequent brain magnetic resonance imaging (MRI) examination performed 1 week later, the thalamus exhibited bilateral circular areas and increased density on T2WI/FLAIR images (white arrow) (E, T1WI; F, T2WI; G, T2WI/FLAIR). A 3-month follow-up cranial MRI revealed slight increases in T1WI and T2WI/FLAIR signals bilaterally in the thalamus, accompanied by internal areas of low density. Surrounding this region, a circular region with 2 areas of low signals was observed, along with white matter demyelination (white arrow) (H, T1WI; I, T2WI; J, T2WI/FLAIR). T2WI, T2-weighted image; T1WI, T1-weighted image; FLAIR, fluid-attenuated inversion recovery.

iron-containing hemosiderin deposition (Fig. 2H-J). Eight patients underwent electroencephalography examination, 5 of whom displayed diffuse slow wave activity and 3 of whom showed electrical silence.

5. Treatment and outcomes

All patients received anticonvulsive therapy, sedation, and measures to reduce intracranial pressure along with supportive treatments. In 32 patients (94.1%), steroids such as methylprednisolone were administered at 10–30 mg/kg/day for 1–5 days, and all patients received intravenous immunoglobulin (IVIG) at a total dose of 2 g/kg over 2 days. However, no significant difference in mortality rate was observed between the steroid- and IVIG-treated groups ($P>0.05$). The fatal group had a greater rate of mechanical ventilation (7 of 15 vs. 19 of 19, $P<0.05$) and shorter hospital and pediatric intensive care unit stays than the survival group (10.9 days vs. 3.4 days, $P<0.05$). The median duration of hospitalization was 6.7 days.

At discharge, 3 patients had recovered and were able to communicate briefly, 2 exhibited increased muscle

tone, and 13 had altered consciousness, including 2 with ongoing seizure activity.

6. ROC curve analysis

ROC curves were constructed to evaluate the ability of the arterial pH, GCS score, and length of hospital stay to predict ANE (Fig. 3). The area under the ROC curve values for the pH, GCS score, and length of hospital stay were 0.76, 0.75, and 0.96, respectively. The sensitivity and specificity of a pH less than 7.337 were 60.0% and 63.2%, those of a GCS score less than or equal to 5 were 80.0% and 73.7%, and those of a hospital stay shorter than 8 days were 93.3% and 89.5%, respectively (Table 5).

Discussion

The results showed ANE has a high mortality rate, which is marked by a significant rise in various laboratory parameters in the fatal group compared to survivors. These parameters include elevated levels of creatin-

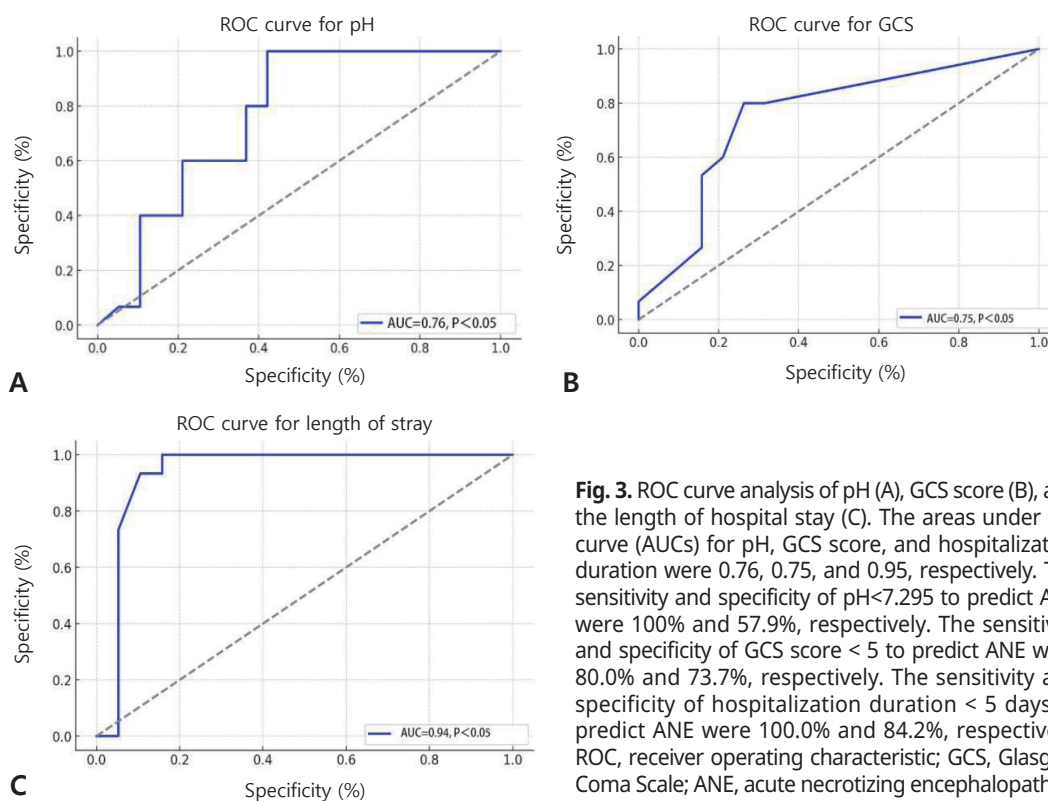


Fig. 3. ROC curve analysis of pH (A), GCS score (B), and length of hospital stay (C). The areas under the curve (AUCs) for pH, GCS score, and hospitalization duration were 0.76, 0.75, and 0.95, respectively. The sensitivity and specificity of pH < 7.295 to predict ANE were 100% and 57.9%, respectively. The sensitivity and specificity of GCS score < 5 to predict ANE were 80.0% and 73.7%, respectively. The sensitivity and specificity of hospitalization duration < 5 days to predict ANE were 100.0% and 84.2%, respectively. ROC, receiver operating characteristic; GCS, Glasgow Coma Scale; ANE, acute necrotizing encephalopathy.

Table 5. Analysis of risk factors for acute necrotizing encephalopathy

Items	Cutoff	Sensitivity	Specificity	95% CI	P value
pH	7.295	100.0	57.89	0.876–20.950	0.033
GCS score	5	80.0	73.68	0.021–0.446	0.031
Hospitalization duration (day)	5	100.0	84.21	0.15–0.63	0.001

GCS, Glasgow Coma Scale; CI, confidence interval.

ine, lactate, APTT, TT, IL-6, IL-10, CK, and D-dimer. Furthermore, the fatal group presented with lower GCS scores and diminished arterial pH levels, which may serve as indicative predictive factors for the severity and outcome of ANE.

ANE predominantly affects young children throughout the year, peaking in winter and spring. Consistent with the findings of Wu et al.²⁰ our study revealed that boys had greater susceptibility to ANE than girls did (22 of 34 vs. 12 of 34; 65% vs. 35%). Viruses, particularly influenza A and B, were pivotal in ANE pathogenesis. The pathophysiology of ANE is hypothesized to involve the virus gaining direct entry to the brain, either through traversal of the nasal mucosa, lamina cribrosa, and olfactory bulb or by retrograde axonal transport. Subsequent to the virus-induced cytokine storm, a complex proinflammatory and prothrombotic cascade unfolds. This hyperinflammatory state represents the core pathogenetic mechanism in ANE patients, irrespective of the initiating pathogen. The disease process adversely impacts both the cerebral vasculature and the blood-brain barrier, leading to secondary manifestations such as cerebral edema and necrosis.³ Our laboratory findings revealed increased inflammatory markers, lactate, creatinine, CK, and D-dimer and decreased GCS scores and arterial pH. These findings underscore the role of the "cytokine storm" in ANE pathogenesis, potentially contributing to increased BBB permeability and systemic manifestations such as liver dysfunction and MOF.²¹

The imaging features of ANE include multifocal, symmetric brain lesions predominantly in the thalamus, basal ganglia, and brainstem. Bilateral thalamic involvement is a distinctive feature of ANE.^{1,13} MRI reveals high-intensity signals on T2WI, hypointensity signals on T1WI, high signals on diffusion-weighted imaging and T2 fluid FLAIR and low signals on apparent diffusion coefficient maps.²² In the middle stage, intracranial edema diminishes, with potential hemorrhage and necrosis in both white and gray matter.^{1,23,24} During the recovery phase, iron-containing hemosiderin deposition, cyst formation and brain atrophy occur.^{13,25}

Previous studies have indicated a relationship between higher mortality rates in ANE patients and lower GCS scores.^{26,27} In our study, the fatal group had a lower arterial blood pH than the survival group, and $\text{pH} \leq 7.295$ had a sensitivity of 100% and specificity of 57.9% for predicting mortality ($P < 0.05$). Severe consciousness disorders were strongly correlated with poor outcomes in ANE patients, with the GCS serving as a critical prognostic marker. This finding underscores the significance of the pH and GCS score in assessing ANE severity and prognosis.

To date, no definitive therapeutic interventions have

been advocated for ANE. However, intensive care, symptomatic treatment, empirical antiviral therapy, and the administration of immunomodulatory agents have been experimented with in the majority of cases. Given the pathogenesis of ANE, characterized primarily by hypercytokinemia secondary to varied viral infections and mediated through immune mechanisms, immunomodulatory interventions—particularly those aimed at suppressing cytokine production—hold promise for enhancing patient outcomes in ANE. The use of intravenous glucocorticoids, immunoglobulins, and plasma exchange is theoretically supported by the underlying pathophysiology of ANE. Certain studies have documented that high-dose methylprednisolone and IVIG therapy, followed by plasmapheresis, correlates with a more favorable prognosis.^{5,20,22} Conversely, another investigation reported an adverse outcome in patients treated with steroids.²⁸ Yet another study found that low-dose methylprednisolone therapy was instrumental in significantly ameliorating the clinical condition.²⁹ So far, there has been no consensus on whether we should prescribe steroids to patients with ANE, as well as the dosage, timing, and the duration. Although several treatments are recommended, such as antiviral therapy, corticosteroids, IVIG, and therapeutic plasma exchange,³⁰⁻³² currently, it is still challenging to administer standardized therapeutic protocols for ANE in clinical practice. The efficacy of antiviral drugs, such as oseltamivir, in reducing neurological complications and improving influenza prognosis remains unclear. In our study, despite the administration of oseltamivir, IVIG, and steroids, the mortality rate remained high at 55.9%, with no significant difference in the mortality rate between the death and survival groups. The use of immune modulation therapies, such as steroids, intravenous immunoglobulins, plasmapheresis, and decompressive craniectomy, did not affect the mortality rate in the survival and fatal groups.

This study has several limitations. As a single-center study with a limited patient cohort, the generality of our findings is of concern. Additionally, our data collection was based on routinely documented patient records, which may have inadvertently excluded essential variables that are not commonly recorded. Moreover, the small sample size restricted to perform robust multi variable analyses or develop predictive models that would have provided deeper insights into ANE progression and treatment efficacy.

In summary, our research identified the GCS score, arterial pH, and length of hospital stay as predictive factors for ANE. Our present study emphasized the importance of effective therapy for ANE patients due to its high morbidity and mortality. Clinicians should be

vigilant for signs such as fever, convulsions, and altered consciousness, as prompt diagnosis and treatment are imperative for improved outcomes. Future studies are required to identify relevant biomarkers for a deeper understanding of ANE and to assess the long-term impacts and treatment efficacy in larger patient cohorts.

Footnotes

Conflicts of interest: No potential conflict of interest relevant to this article was reported.

Funding: This study received no specific grant from any funding agency in the public, commercial, or not-for-profit sectors.

Author contribution: Conceptualization: XL, SY; Methodology: XL, SY; Formal Analysis: QD, YW, HZ; Investigation: QD, YW, HZ; Writing-Original Draft: HZ; Writing-Review & Editing: SY, XL

ORCID:

Huiling Zhang  <https://orcid.org/0009-0003-3985-6025>

Yilong Wang  <https://orcid.org/0000-0002-7833-9990>

Qianyun Ding  <https://orcid.org/0000-0003-0907-3057>

Xuekun Li  <https://orcid.org/0000-0002-6985-6363>

Sheng Ye  <https://orcid.org/0000-0003-2201-0261>

References

1. Mizuguchi M, Abe J, Mikkaichi K, Noma S, Yoshida K, Yamanaka T, et al. Acute necrotising encephalopathy of childhood: a new syndrome presenting with multifocal, symmetric brain lesions. *J Neurol Neurosurg Psychiatry* 1995;58:555-61.
2. Shukla P, Mandalla A, Elrick MJ, Venkatesan A. Clinical manifestations and pathogenesis of acute necrotizing encephalopathy: the interface between systemic infection and neurologic injury. *Front Neurol* 2021;12:628811.
3. Kidokoro H. Acute necrotizing encephalopathy: a disease meriting greater recognition. *AJNR Am J Neuroradiol* 2020;41:2255-6.
4. Mizuguchi M, Yamanouchi H, Ichiyama T, Shiomi M. Acute encephalopathy associated with influenza and other viral infections. *Acta Neurol Scand Suppl* 2007;186:45-56.
5. Poojari VS, Shah I, Shetty NS. Acute necrotising encephalopathy of childhood secondary to rotaviral diarrhoea. *Indian Pediatr* 2021;58:491.
6. Khan M, Bhattarai S, Boyce TG, Hayek RA, Zhadanov SI, Hooper EE, et al. Acute necrotizing encephalopathy associated with coronavirus disease 2019 in an infant. *J Pediatr* 2022;247:160-2.
7. Stevanovic V, Barusic Z, Viskovic K, Rode OD, Tesovic G. Acute necrotizing encephalopathy of childhood associated with human herpes virus 6 in Croatia. *Neurol Sci* 2019; 40:639-41.
8. Agrawal V, Chaudhary S, Pandey S. Acute necrotising encephalopathy: a rare complication providing a clue for the outbreak of H1N1 among medical students in Kanpur, India. *Trop Doct* 2023;53:205-6.
9. Wang PY, Yang MT, Liang JS. Acute necrotizing encephalopathy caused by SARS-CoV-2 in a child. *Pediatr Neonatol* 2022;63:642-4.
10. Kirton A, Busche K, Ross C, Wirrell E. Acute necrotizing encephalopathy in caucasian children: two cases and review of the literature. *J Child Neurol* 2005;20:527-32.
11. Zhang J, Liu J, Wang J, Gan J. Anti-NMDAR encephalitis secondary to acute necrotizing encephalopathy caused by herpes simplex virus infection in infants: case series. *Clin Neurol Neurosurg* 2023;233:107955.
12. Hu Y, Tian Z, Zhao B, Dong C, Cao L. A novel variation in RANBP2 associated with infection-triggered familial acute necrotizing encephalopathy. *Neurol Sci* 2022;43:3973-7.
13. Wu X, Wu W, Pan W, Wu L, Liu K, Zhang HL. Acute necrotizing encephalopathy: an underrecognized clinicoradiologic disorder. *Mediators Inflamm* 2015;2015:792578.
14. Lin YY, Lee KY, Ro LS, Lo YS, Huang CC, Chang KH. Clinical and cytokine profile of adult acute necrotizing encephalopathy. *Biomed J* 2019;42:178-86.
15. Sun Y, Zou Y, Wang H, Cui G, Yu Z, Ren Z. Immune response induced by novel coronavirus infection. *Front Cell Infect Microbiol* 2022;12:988604.
16. Arul JN, Madhavan S, Krishnan V, Krishnamoorthy V. Fatal H1N1-related acute necrotising encephalopathy in an adult. *BMJ Case Rep* 2020;13:e235264.
17. Ichiyama T, Endo S, Kaneko M, Isumi H, Matsubara T, Furukawa S. Serum cytokine concentrations of influenza-associated acute necrotizing encephalopathy. *Pediatr Int* 2003;45:734-6.
18. Ong SCL, Nur Azidawati AH, Liew YH, Anita S. Acute necrotising encephalopathy of childhood: a review of two cases. *Med J Malaysia* 2017;72:311-3.
19. Neilson DE. The interplay of infection and genetics in acute necrotizing encephalopathy. *Curr Opin Pediatr* 2010;22:751-7.
20. Wu L, Peng H, Jiang Y, He L, Jiang L, Hu Y. Clinical features and imaging manifestations of acute necrotizing encephalopathy in children. *Int J Dev Neurosci* 2022;82:447-57.
21. Qin N, Wang J, Peng X, Wang L. Pathogenesis and management of acute necrotizing encephalopathy. *Expert Rev Neurother* 2023;23:641-50.
22. Sarigecili E, Ucar HK, Havali C, Cansu A, Aydin K. Acute necrotizing encephalopathy associated with RANBP2 mutation: value of MRI findings for diagnosis and intervention. *Acta Neurol Belg* 2023;123:571-82.
23. Biswas A, Varman M, Gunturi A, Yoganathan S, Gibikote S. Teaching neuroimages: acute necrotizing encephalopathy of childhood: neuroimaging findings. *Neurology* 2018;90: e177-8.
24. Li H, Sun C, Chi S, Wang Y, Wu L, Qin X. Use of MRI in the diagnosis and prognosis of acute necrotizing encephalopathy.

- phalopathy in a Chinese teenager: a case report. *Medicine (Baltimore)* 2019;98:e17797.
25. Tabarki B, Thabet F, Al Shafi S, Al Adwani N, Chehab M, Al Shahwan S. Acute necrotizing encephalopathy associated with enterovirus infection. *Brain Dev* 2013;35:454-7.
 26. Li KC, Wang LJ, Liu G, Jin P, Wang YQ, Zhang T, et al. [Analysis of 39 children with acute necrotizing encephalopathy]. *Zhonghua Er Ke Za Zhi* 2021;59:582-7.
 27. Chow CK, Ma CKL. Presentation and outcome of acute necrotizing encephalopathy of childhood: a 10-year single-center retrospective study from Hong Kong. *J Child Neurol* 2020;35:674-80.
 28. Kim YN, You SJ. A case of acute necrotizing encephalopathy associated with parainfluenza virus infection. *Korean J Pediatr* 2012;55:147-50.
 29. Mariotti P, Iorio R, Frisullo G, Plantone D, Colantonio R, Tartaglione T, et al. Acute necrotizing encephalopathy during novel influenza A (H1N1) virus infection. *Ann Neurol* 2010;68:111-4.
 30. Okajima K, Hayakawa I, Tsuboi N, Shimura K, Ishiguro A, Abe Y. Early therapeutic plasma exchange may lead to complete neurological recovery in moderate to severe influenza-associated acute necrotizing encephalopathy. *Brain Dev* 2022;44:492-7.
 31. Okumura A, Mizuguchi M, Kidokoro H, Tanaka M, Abe S, Hosoya M, et al. Outcome of acute necrotizing encephalopathy in relation to treatment with corticosteroids and gammaglobulin. *Brain Dev* 2009;31:221-7.
 32. Mizuguchi M, Ichiyama T, Imataka G, Okumura A, Goto T, Sakuma H, et al. Guidelines for the diagnosis and treatment of acute encephalopathy in childhood. *Brain Dev* 2021;43:2-31.

How to cite this article: Zhang H, Wang Y, Ding Q, Li X, Ye S. Clinical characteristics and associated factors of pediatric acute necrotizing encephalopathy: a retrospective study. *Clin Exp Pediatr* 2025;68:153-62.